

# COMPUTATIONAL ANALYSIS OF BLENDED WING BODY UAV CONFIGURATION WITH AND WITHOUT FLAPS

<sup>1</sup>Naresh D C, <sup>2</sup>Rekha M, <sup>3</sup>Tejaswini Y, <sup>4</sup>Cheluvraj N, <sup>5</sup>Varshini B V

<sup>1</sup>Asst. Professor, Dept. of Aeronautical Engineering, Dayananda Sagar College of Engineering, Karnataka, India

<sup>2,3,4,5</sup> Students, Dept. of Aeronautical Engineering, Dayananda Sagar College of Engineering, Karnataka, India

\*\*\*

**Abstract** - Blended Wing Body (BWB), as the name indicates it's a mixture of both the wings and therefore the body of the Aircraft, unlike conventional configurations where wings are attached to the fuselage and forms a separate section within the aircraft's structure but within the blended wing body the fuselage and therefore the wings of the aircraft is fused into one entity. This design features a great advantage over the traditional design like reduction of drag, high lift co-efficiency, more capaciousness, significant increase within the cargo space. Over the decades the BWB aircraft is additionally identified as Flying Wing/ Tailless aircraft. BWB may be a futuristic concept aircraft that features a potential to be used commercially. It offers advantages of aerodynamic performance and fuel economy. Our area of interest is primarily focus is on the flow analysis of the Blended wing Body (BWB) and understanding its aerodynamic behavior. During this present study an effort has been made to style a Blended Wing Body (BWB) UAV configuration with and without flaps using solid works 2018 and to conduct different parametric analysis and analyzing it through CFD approach using ANSYS 18.1. Also the development within the lift generation and increase within the L/D ratio are often verified with the previously designed BWB UAV without flaps.

**Key Words:** *Blended Wing Body (BWB), Aerodynamic co-efficient, and CFD Analysis.*

## 1. INTRODUCTION

### 1.0. INTRODUCTION

The Blended Wing Body (BWB) is a hybrid shape that resembles a flying wing, but also it in cooperates features from conventional transport aircraft. This mix offers several advantages over the traditional tube and wing airframe. The Blended Wing Body (BWB) airframe merges efficient high lift wings with a good airfoil shaped body, allowing the whole aircraft to get lift and thus to scale back the dimensions and drag of wings which results in better aerodynamic characteristics. With this we've now received a stage of finding the performance blended wing body of various configurations of an aircraft as per its standards, this project deals with the designing a Blended Wing Body (BWB) UAV with and without flaps and that they are been analyzed at different AOA at different velocities. And also to conduct the various parametric analyses for with flap configuration and analyzing it through CFD approach at different AOA for a constant velocity. Where this process is been administered to see out the flow analysis of Blended Wing Body (BWB) type

at which AOA for a given velocity gives the utmost aerodynamic results.

### 1.1. UNMANNED AERIAL VEHICLE (UAV)

Unmanned aerial vehicles are often defined as any sort of aerial vehicle without a person's pilot on board. UAV's are often of varied types including rotor wing aircraft, fixed wing aircraft, etc. Here we refer aerial unmanned vehicles to fixed-wing aerial vehicles. UAV's are controlled by human pilots from a foreign distance or are often fully autonomous. During this case, the auto-piloting software is integrated in on-board computers. The flight paths for a selected mission are often pre-programmed into the memory of the onboard computer. They perform many functions including search operations after natural disasters, photography, scrutinizing global climate change etc. they will also perform certain military operations like surveillance, reconnaissance and targeted attacks.

### 1.2. BLENDED WING BODY CONFIGURATION

Blended Wing Body (BWB) is an idea where fuselage is combined with wing and tail to become a single entity where figure 1.1 indicates a typical BWB UAV. Blended wing body is a hybrid of conventional and the flying wing aircraft. The body is designed to have a shape of an airfoil and sensibly streamlined with the wing to have a preferred platform. The major transformation of this BWB concept is the way it generates lift. Conventional aircraft obtains its lift from its wings. However, BWB aircraft attains lift from its wings along with its fuselage. The control surfaces of the wing are located along the leading and trailing edges of the wing and on the winglets. The number of control surfaces can differ from 14 to 20 depending on its design. The BWB has low noise signature, furthermore, due to reduced fuel burn BWB emanates the pollutants in traces. Misery conducted a research to determine the airframe with the least noise characteristics, out of 96 aircraft configurations, the discrete BWB airframe obtained the highest score of 64.3% compared to the conventional wing. To conclude, the BWB aircraft configuration has the ability to provide a great number of benefits through its structural concepts, such as its aerodynamically low interface drag, high lift-to-drag ratio, structurally favorable span loading, and the reduction of greenhouse emissions.



Figure1.1: Typical BWB UAV

### 1.3. HIGH LIFT DEVICES

In aircraft design, a high-lift device is an element or mechanism on the wing of an aircraft that augments the amount of lift produced by the wing. The device may be a fixed component, or a movable mechanism which is installed when it is necessary. Wing flaps and slats are the common movable high-lift devices. Leading-edge slots, leading edge root extensions, and boundary layer control systems are some of the fixed devices. Out of these high lift devices, flaps are of our interest. Flaps are a type of high-lift devices used to decrease the stalling speed of an aircraft wing at a given weight. Flaps are generally mounted on the wing trailing edges in case of fixed-wing aircraft. Flaps are typically operated to trim down the take-off and the landing distance. Flaps will essentially increase drag, so they are retracted when it's not needed. Increasing the wing flaps increases the curvature of the wing i.e. the camber, thus increasing the maximum lift coefficient or the upper limit to the lift a wing can produce. This permits the generation of the required lift of an aircraft, reducing the minimum speed at which the aircraft will safely maintain flight also known as the stalling speed. It is also seen that increase in camber will produce increase in drag, and that is beneficial during approach and landing as it slows down the aircraft.

### 1.4. TYPES OF FLAPS

Different types of flaps are as follows. Figure 1.2 shows different types of flap.

- Plain Flaps
- Split Flaps
- Slotted Flaps
- Fowler Flaps
- Krueger Flaps
- Zap Flaps

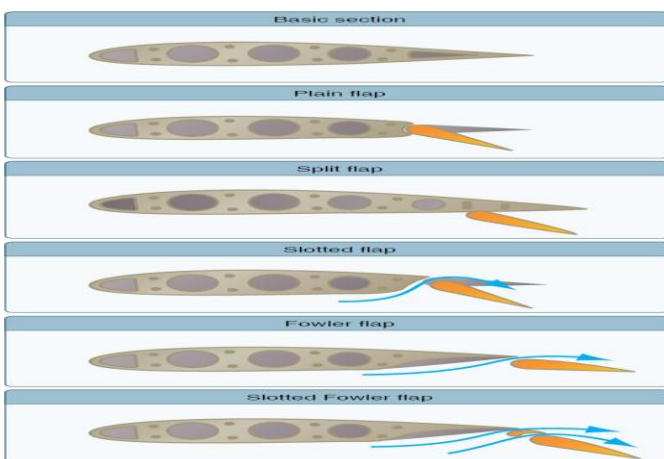


Figure1.2: Different types of flaps

### 1.5. EFFECT OF FLAPS ON THE AIRCRAFT

The below figure 1.3 indicates the effect of flaps

- Flaps increase lift and thereby reducing stalling speed, and it enables take-off at lower air speed.
- Shorter ground run, reduction in rate of climb due to increase in drag.
- Lower take-off and landing speeds.
- Less wear and tear on brakes.

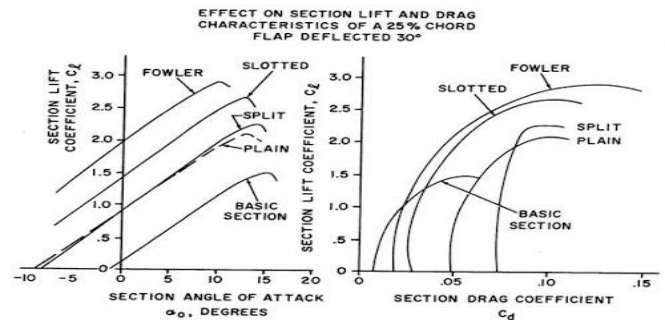


Figure1.3: Effect of flaps

## 2. LITERATURE SURVEY

### 2.1. LITERATURE SURVEY

Shreya G, Vinitha G, Isha G, Shreya M<sup>[1]</sup>, "Computational Analysis Blended wing Body With And Without Flaps", on 2020, the flaps increase the drag coefficient of an aircraft due to higher induced drag, it can be seen from the results that as the angle of attack increases, at higher angles of attack (15°), the drag values of both the design becomes equal. Simultaneously, lift value of with-flaps design is higher than without-flaps design. Since, drag is almost equal in both the designs, but lift value is more when flaps are used, hence the L/D ratio increases to a much greater values at higher angles of attack (around 22.69% increase at v = 25 m/s).

Pranav Mahamuni, A. Kulkarni, Yash Parikh<sup>[2]</sup>, "Aerodynamic Study of Blended Wing Body", January 2014, The motivation of this paper was concluded that BWB configuration has not only high L/D ratio but also low fuel consumption and increased payload carrying capacity than conventional aircraft.

Martin Masereel, <sup>[3]</sup> the title of the paper is "Improvement of the aerodynamic behavior of a blended wing body unmanned aerial vehicle", the journal was published on 2016, on University of Liege. The aim of this research paper where, a sensitivity analysis on the Reynolds was performed to ascertain if a future structure test campaign on a reduced size model might be possible. Trends showed that it had been safe to research the UAV at different Reynolds number when the presence of thrust was ignored. The introduction of thrust led to some dependencies on the Reynolds pointing to the very fact that a structure test should be performed cautiously. This is often done by varying the taper ratio and therefore the sweep angle of the wing also because the taper ratio, sweep angle and height of the winglet.

## 2.2 MOTIVATION FOR THE RESEARCH WORK

Several research studies indicate that the Blended Wing Body (BWB) concept offers a big performance improvement compared to traditional civil transport aircraft because of its efficient Aerodynamic configuration. The Blended Wing Body (BWB) represents a paradigm shift within the design of aircraft. The design offers immense aerodynamics and environment benefits. Few papers are collected and literature survey has been done by studying the paper. Because of the advancements in current technology of UAV design and its large scope of application in various fields under various environments, it's important to enhance the performance of such UAV's through innovative ideas for satisfying future requirements. Thus, undertaking a work on UAV design and performance and application of BWB concept gave an excellent motivation for us to probe further in UAV technology. Increasing environmental concerns and fuel prices motivate the study of other, un-conventional aircraft configurations. One such example is that the blended-wing-body configuration, which has been shown to possess several advantages over the traditional tube-and-wing aircraft configuration.

## 3. PROBLEM STATEMENT AND OBJECTIVES

### 3.1. PROBLEM DESCRIPTION

To design, analyze a typical BWB UAV configuration with and without flaps for low Reynolds number and low speed conditions computationally. And to perform the different parametric analysis of BWB UAV for with flap configuration at a different AOA for a constant velocity.

### 3.2. OBJECTIVES OF THE PROJECT

To perform CFD Analysis of BWB UAV with flaps and without flaps and compare their aerodynamic coefficients.

- ✓ To select an appropriate airfoil that satisfies our design requirements by analyzing the selected airfoils suitable for BWB UAV design on XFLR.
- ✓ To design models of Blended Wing Body UAV configuration with and without flaps using Solid works 2018.
- ✓ To analyze both the designed models of BWB UAV by using ANSYS 18.1.
- ✓ To validate that the proposed BWB UAV with flaps concept offers better aerodynamic characteristics as compared to BWB UAV without flaps.
- ✓ And perform different parametric analysis for BWB UAV for with flap configuration.

## 4. METHODOLOGY

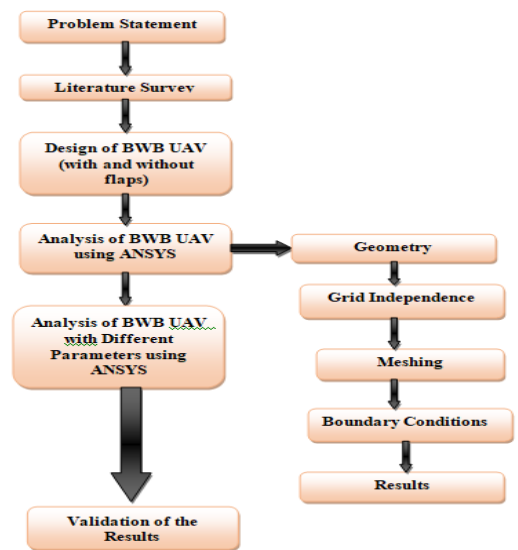


Figure4.1: Design Methodology

## 5. AIRFOIL ANALYSIS AND SELECTION

### 5.1. SELECTED AIRFOILS FOR XFLR ANALYSIS

The majority of the lift is produced by the center body in case of BWB UAV. Therefore it was necessary to choose a high lift airfoil at the root chord. Four high-lift airfoils suitable for blended wing body were chosen and they were analyzed on XFLR and the necessary graphs were plotted. The airfoils that were chosen include S1223, E422, E423, FX74.

### 5.2. SELECTION OF AIRFOIL FOR THE ROOT CHORD

Lift and drag coefficients were the main criteria used in order to select the airfoil for the root chord. S1223 was thus selected as it had a high lift coefficient as well as a low drag coefficient value, when compared to the other 3 airfoils.

#### 5.2.1. LIFT COEFFICIENT ( $C_l$ ) vs. ANGLE OF ATTACK (AOA)

The lift coefficient,  $C_l$  vs  $\alpha$  for four different airfoils is as shown in Figure 5.1. From the graph, it is observed that each of the airfoil show the distinctive nature in lift at different angle of attacks (AOA). When the airfoil S1223 is compared with the other three airfoils, it shows linear increase in the lift and also has high lift co-efficient at low angle of attack i.e. at  $9.75^\circ$  having a better performance.

#### 5.2.2. DRAG COEFFICIENT ( $C_d$ ) vs. ANGLE OF ATTACK (AOA)

The drag coefficient  $C_d$  has been plotted vs. different angle of attacks (AOA), as shown in the Figure 5.2. Due to the flow separation the drag increases with increase in angle of attack. From the Figure 5.7, the obtained drag coefficient for S1223 airfoil is lesser than other three airfoils.

#### 5.2.3. LIFT COEFFICIENT vs. DRAG COEFFICIENT ( $C_l$ vs. $C_d$ )

The curve shown in figure 5.3 has two important features viz. minimum drag coefficient ( $C_{dmin}$ ) and lift coefficient ( $C_l$ )



corresponding to ( $C_{dmin}$ ). From the Figure 5.3, S1223 airfoils have large drag at higher angle of attack and can generate higher lift compared to other three airfoils.

**5.3. SELECTION OF AIRFOIL FOR THE TIP CHORD**

MH45 has low moment coefficient of  $C_{Mc/4}=0.0145$ <sup>[2]</sup>. This was important because for the chosen configuration required the airfoils to produce minimal negative  $C_M$  values to make it possible to obtain a positive  $C_M$  for the entire wing. This airfoil produces a relatively high  $C_{LMAX}$  of 1.28 at Reynolds number 100000. When it is used at the tip of the wing, it provides aerodynamic twist. Therefore, MH45 is chosen at the tip chord.

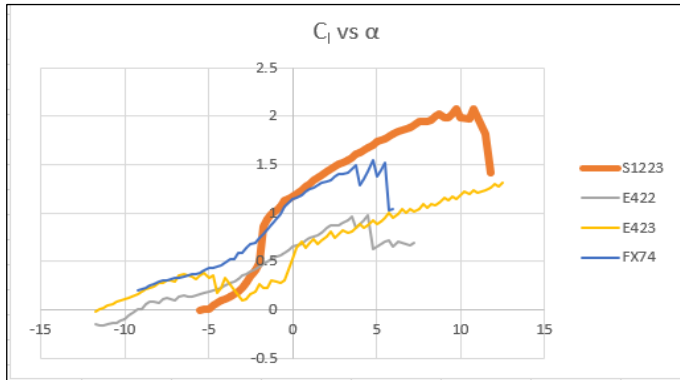


Figure 5.1:  $C_l$  vs.  $\alpha$

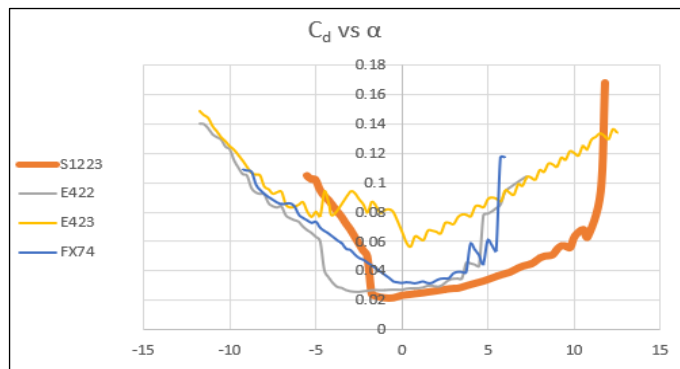


Figure 5.2:  $C_d$  vs.  $\alpha$

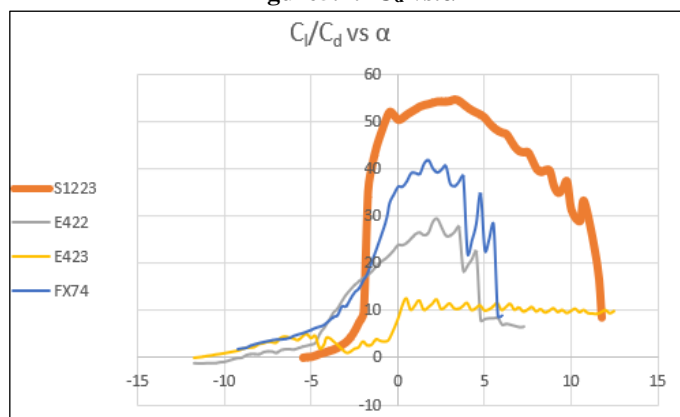


Figure 5.3:  $C_l/C_d$  vs.  $\alpha$

**6. DESIGN AND ANALYSIS OF BWB UAV**

**6.1. DESIGN OF BWB UAV**

Based on the defined objective of the project, we have focused on the geometrical aspects of BWB aircraft. Through

literature survey we have selected the BWB UAV design configuration from Sanjiv Paudel, Shailendra Rana, Saugat Ghimire, Kshitiz Kumar Subedi, Sudip Bhattarai, "Aerodynamic and Stability Analysis of Blended Wing Body Aircraft", 2016. Using MH45 as the tip chord and S1223 as the root chord we have designed BWB UAV with flaps and without flaps whose specifications are given in Table 6.1. The design of BWB UAV without flaps is as shown in Figure 6.1.

**Table 6.1.-: Specifications of Designed BWB UAV**

SPECIFICATIONS	
Wing Span (m)	0.36
Root Chord(m)	0.152
Tip Chord(m)	0.02
Taper Ratio	0.13
Sweep angle	33°
Dihedral angle	0°

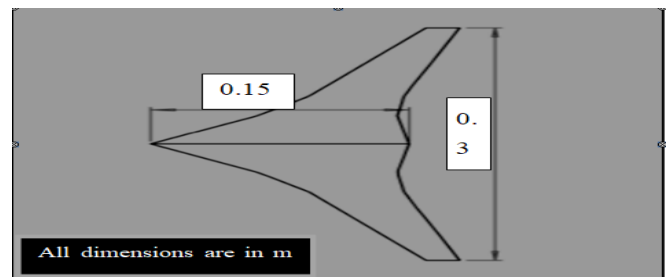


Figure 6.1: Dimensions of BWB UAV without flaps

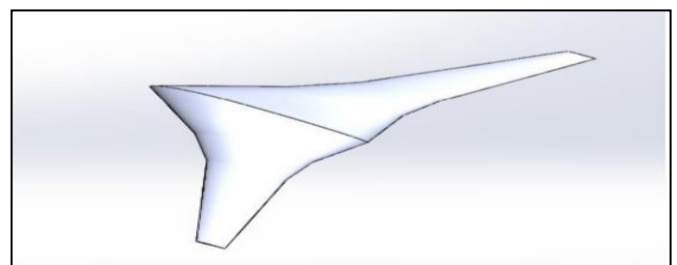


Figure 6.2: Isometric view of BWB UAV without flaps

**Table 6.2:- Flap dimension**

Root chord of flap (m)	Tip chord of flap (m)	Span (m)	Deflection angle
0.0214	0.014	0.026	0

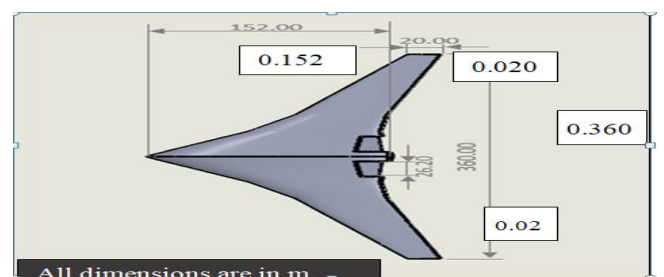


Figure 6.3: Dimensions of BWB UAV with flaps

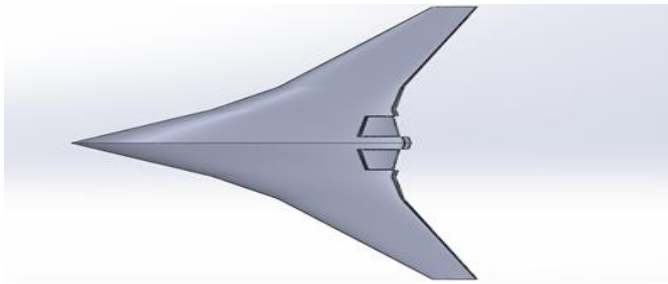


Figure6.4: Top view of BWB UAV with flaps

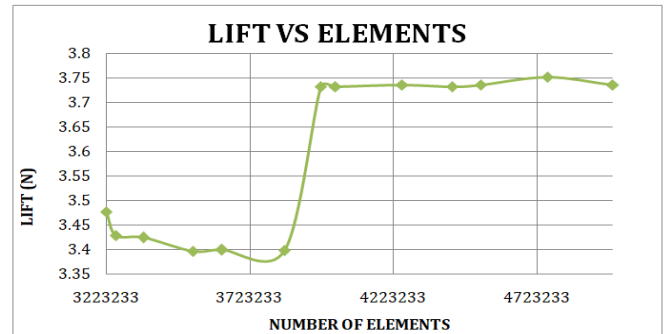


Figure6.7: Lift vs. Number of elements for with flaps

Table 6.3:- Node and Element details of BWB UAV

	WITHOUT FLAPS	WITH FLAPS
<b>NODES</b>	<b>249645</b>	<b>725875</b>
<b>ELEMENTS</b>	<b>1348002</b>	<b>3970060</b>

6.2. ANALYSIS OF BWB UAV

6.2.1. GEOMETRY

The file exported from Solid works is imported into geometry of ANSYS FLUENT and the enclosure is created of size 1.5m x 1.5m x 1.5m. The enclosure is as shown in Figure 6.5.

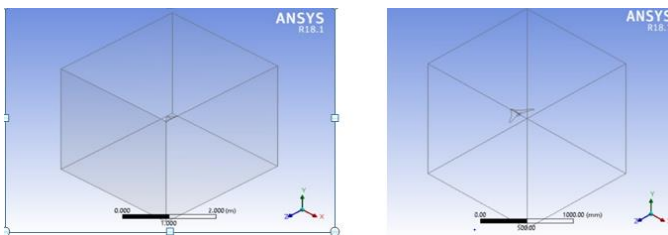


Figure6.5: Enclosure

6.2.2. MESHING

Meshing for both the models are done using edge sizing and face meshing operations. The number of elements and the corresponding number of nodes are selected based on grid independence study. Both the models contain tetrahedral elements.

6.2.2.1. GRID INDEPENDENCE STUDY

Grid independence study is important in FLUENT for a certain geometry to get accurate answers. This is done by varying the mesh size from course to fine, and checking the output result for each mesh. When varying the mesh doesn't affect the result much we can stop and select that minimum mesh size for our final solution output.

- Grid independent study was done for both the designed models at 20m/s velocity and at 0° angle of attack. .
- Number of divisions in edge sizing operation was varied from 20 to 80 divisions in steps of 5.
- Values of lift were plotted against number of elements for both the designs as shown in figures 6.6 and 6.7.
- The number of elements is marked in the Figures 6.6 and 6.7, after which there are no significant changes in the values.

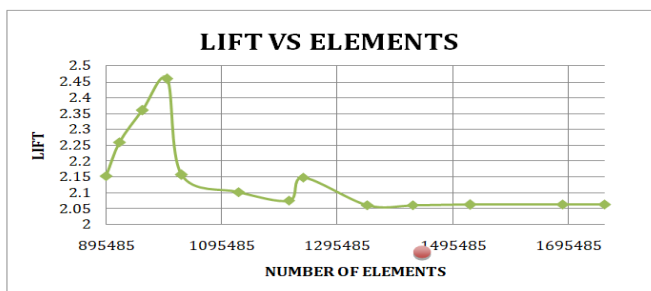


Figure6.6: Lift vs. Number of elements for without flaps

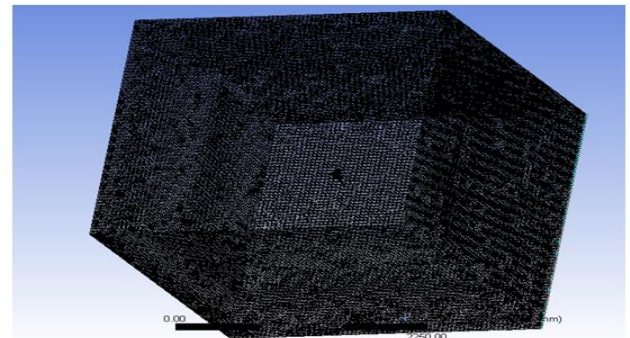


Figure6.8: Meshing over the BWB UAV without flap

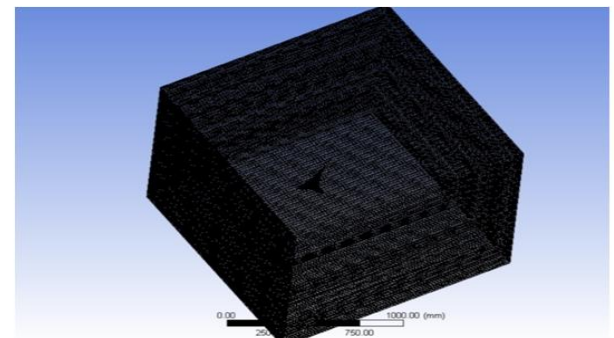


Figure6.9: Meshing over the BWB UAV with flaps model

6.2.3. BOUNDARY CONDITIONS

Table 6.4: Boundary Conditions

ZONE	TYPE
INLET	VELOCITY
OUTLET	PRESSURE
WALLS	WALL
BWB	WALL

Table 6.5: Solver Details

SOLVER DETAILS	
SOLVER	PRESSURE BASED
TIME	STEADY
MODEL	SPALART ALLMARAS
MATERIAL (FLUID)	AIR
SOLUTION INITIALIZATION	STANDARD

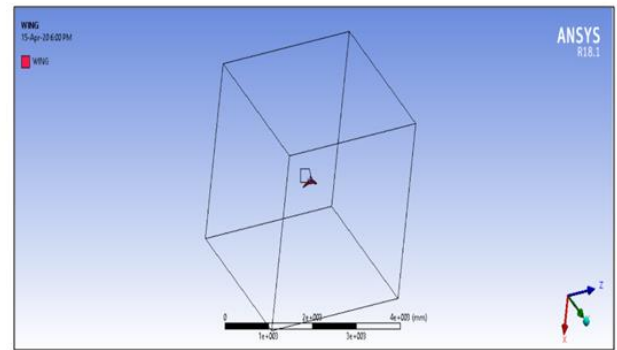


Figure6.13: BWB

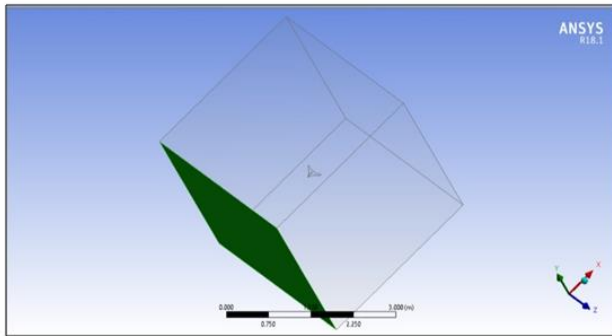


Figure6.10: Inlet

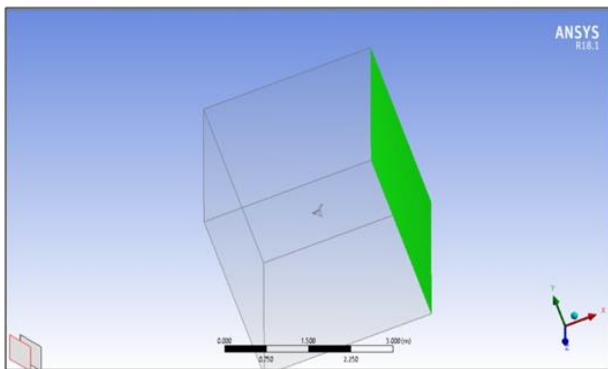


Figure6.11: Outlet

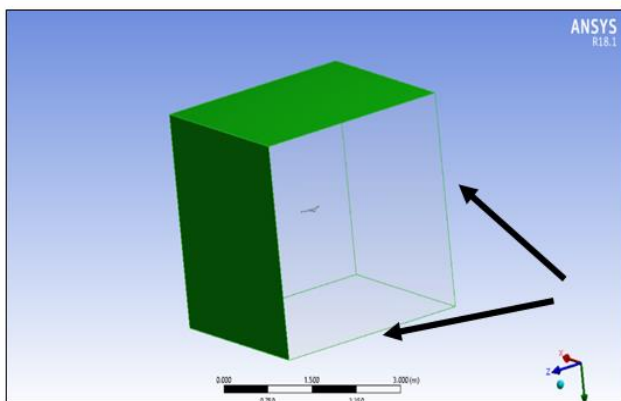


Figure6.12: Walls

## 7. RESULTS AND DISCUSSIONS

Analysis of the two designs (with and without flaps) were done at five different velocities (10,15, 20,25,30m/s) and at 5 different angles of attack (-5°,0°, 5°, 10°, 15°).

### 7.1. NUMERICAL RESULTS OF BWB UAV WITHOUT FLAPS

The contour of pressure magnitude obtained for various velocities at different angles of attack from CFD simulations are shown in Figures 7.1 to 7.5. At -5° angle of attack, there is very low pressure on the surfaces of the aircraft.

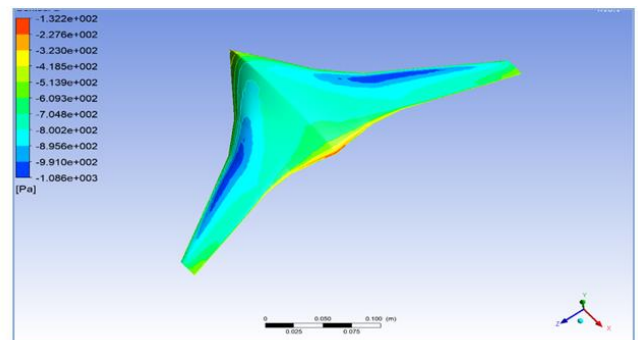


Figure7.1: Pressure contour at -5 ° angle of attack at 10m/s

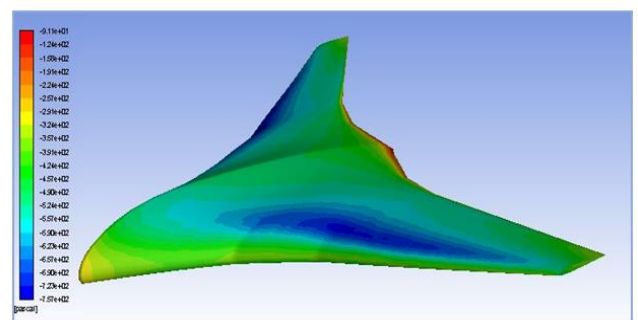


Figure7.2: Pressure contour at -5 ° angle of attack at 15m/s

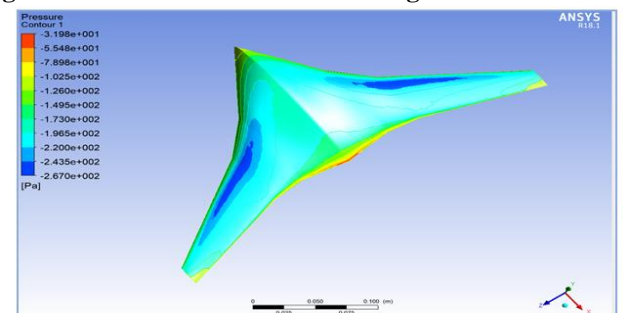


Figure7.3: Pressure contour at -5 ° angle of attack at 20m/s



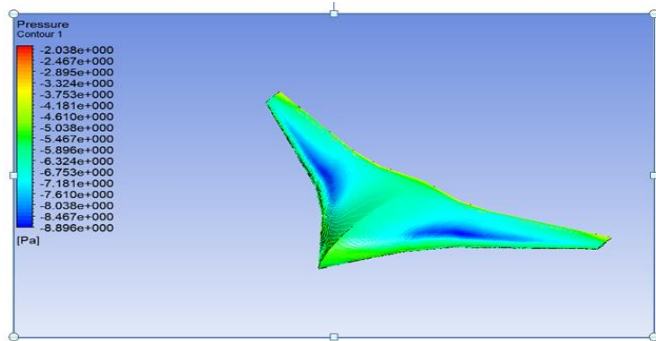


Figure7.4: Pressure contour at -5° angle of attack at 25 m/s

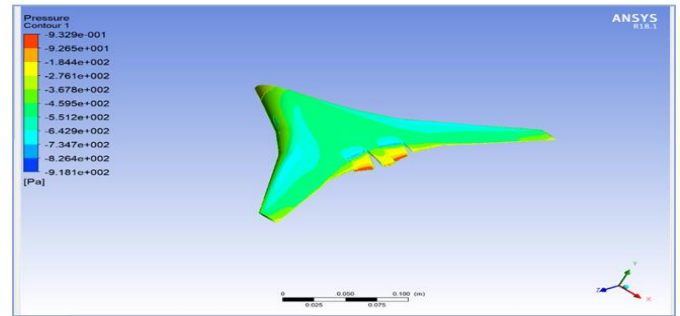


Figure7.6: Pressure contour at -5° angle of attack at 15 m/s

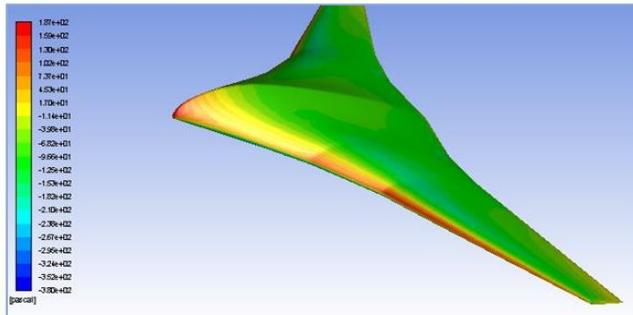


Figure7.5: Pressure contour at -5° angle of attack at 30 m/s

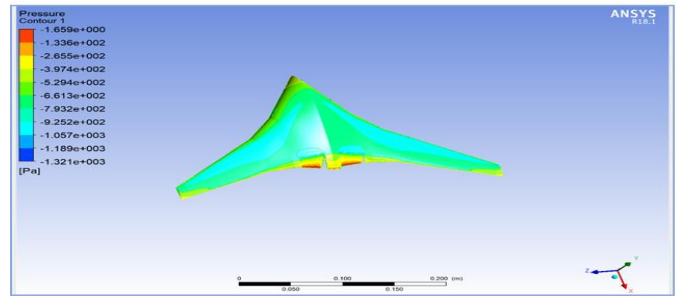


Figure7.7: Pressure contour at -5° angle of attack at 20 m/s

At -5° angle of attack at 30m/s velocity the pressure is higher at the lower surface and on the leading edge of the aircraft as shown in the Figure 7.5. The maximum pressure obtained is 187 Pa. For all the positive angles of attack, it is found that pressure is higher at the leading edge and the bottom surface of the wing. Larger the angle of attack, greater is the difference between the lower and upper surface. It is also seen that pressure difference is much larger on the front edge, while on rear edge it was much lower, thus indicating that the lift force of the aircraft is mainly generated from the front edge.

### 7.2 NUMERICAL RESULTS AND DISCUSSION WITH FLAPS

The contour of pressure magnitude obtained for various velocities at different angles of attack from CFD simulations are shown in figures 7.6 to 7.10.

It is seen that flaps design has a higher pressure difference between the lower and upper surface, when compared to without flaps design. Hence, there is more lift generated when flaps are used. Also, as the angle of attack increases, the pressure difference also increases just like the previous design.

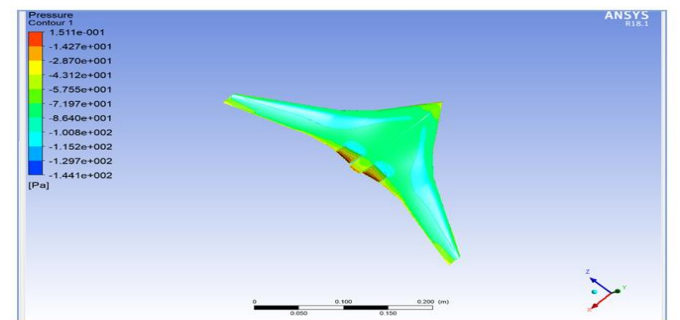


Figure7.8: Pressure contour at -5° angle of attack at 25 m/s

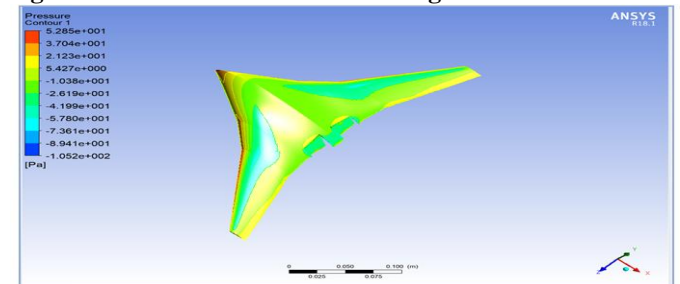


Figure7.9: Pressure contour at -5° angle of attack at 30 m/s

At -5° angle of attack at 30 m/s velocity, the pressure is higher at the bottom surface of the aircraft, relatively high at the trailing edge of the aircraft and also on the upper surface of the flaps. The maximum pressure obtained is 0.151 Pa.

### 7.3. CALCULATIONS AND RESULTS

The lift and drag values are obtained through analysis and the corresponding coefficients of lift and drag are calculated and plotted against angle of attack.

In blended wing body the wings along with fuselage will act as an aerodynamic entity unlike conventional wings.

Surface Area  $S = 0.0248 \text{ m}^2$ ; Density of Air  $\rho = 1.225 \text{ Kg/m}^3$ ; Velocity  $v = 10 \text{ m/s}$ ;

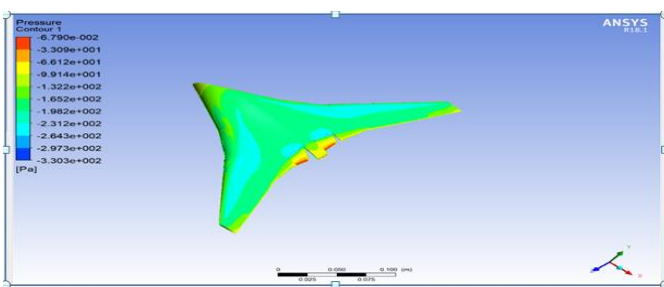


Figure7.6: Pressure contour at -5° angle of attack at 10 m/s

Using their respective formulas, coefficient of lift and coefficient of drag are calculated. At -5° Angle of attack and 10 m/s velocity for BWB UAV **without flaps**,

$$L = -0.2726 \text{ N}; \quad D = 0.0367 \text{ N};$$

$$C_L = \frac{2L}{\rho \cdot v^2 \cdot S} = \frac{2 \cdot (-0.2726)}{1.225 \cdot 10^2 \cdot 0.0248} = -0.1794$$

$$C_D = \frac{2D}{\rho \cdot v^2 \cdot S} = \frac{2 \cdot 0.0367}{1.225 \cdot 10^2 \cdot 0.0248} = 0.0241$$

The Table 7.1 summarizes the lift and drag coefficients calculated for without flaps design, for all angles of attack at 10 m/s velocity.

**Table 7.1:- C<sub>L</sub> and C<sub>D</sub> values at different angle of attack at 10m/s (without flaps)**

WITHOUT FLAPS (v = 10 m/s)					
AOA	Lift	C <sub>L</sub>	Drag	C <sub>D</sub>	C <sub>L</sub> /C <sub>D</sub>
-5°	-0.2726	-0.1794	0.0367	0.0241	-7.329
0°	0.3576	0.2354	0.0266	0.0175	13.443
5°	0.5078	0.3342	0.0369	0.0242	13.761
10°	0.7065	0.4651	0.039	0.0256	18.115
15°	0.77	0.5069	0.05	0.0329	15.4

At -5° Angle of attack and 10 m/s velocity for BWB UAV **with flaps**, L = -0.225 N; D = 0.0388 N;

$$C_L = \frac{2L}{\rho \cdot v^2 \cdot S} = \frac{2 \cdot (-0.225)}{1.225 \cdot 10^2 \cdot 0.0248} = -0.148$$

$$C_D = \frac{2D}{\rho \cdot v^2 \cdot S} = \frac{2 \cdot 0.0388}{1.225 \cdot 10^2 \cdot 0.0248} = 0.0255$$

The Table 7.2 summarizes the lift and drag coefficients calculated for with flaps design, for all angles of attack at 10 m/s velocity.

**Table 7.2:- C<sub>L</sub> and C<sub>D</sub> values at different angle of attack at 10m/s (with flaps)**

WITH FLAPS (v = 10 m/s)					
AOA	Lift	C <sub>L</sub>	Drag	C <sub>D</sub>	C <sub>L</sub> /C <sub>D</sub>
-5°	-0.225	0.1481	0.0388	0.0255	-5.977
0°	0.4809	0.3165	0.0348	0.0229	13.7489
5°	0.7426	0.4888	0.0465	0.0306	15.7299
10°	0.8619	0.5674	0.047	0.0309	16.9077
15°	0.9348	0.6154	0.0527	0.0346	17.5385

The Figures 7.11 and 7.12 shows the comparison of lift and drag coefficients of both the designs (with and without flaps). It is seen that C<sub>L</sub> and C<sub>D</sub> is more for the with flaps design. The maximum value of C<sub>L</sub> obtained is 0.6154 and the corresponding C<sub>D</sub> value is 0.0346 for with flaps design, while the maximum C<sub>L</sub> and C<sub>D</sub> values for without flaps design are 0.5069 and 0.0329 respectively.

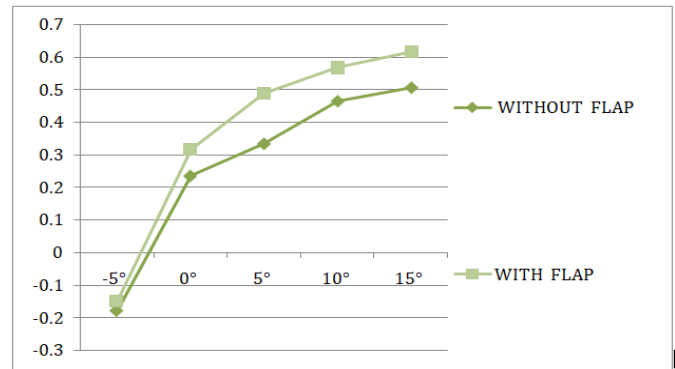


**Figure 7.10: C<sub>L</sub> vs. α at 10 m/s velocity**

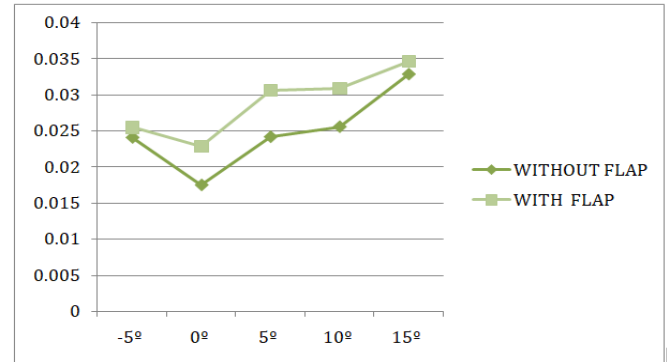


**Figure 7.11: C<sub>D</sub> vs. α at 10 m/s velocity.**

**At 15m/s Velocity**

The calculated coefficients of lift and drag values at 15 m/s velocity for without flaps and with flaps are as shown in the Table 7.3 and Table 7.4 respectively. The Figures 7.13 and 7.14 shows the comparison of both the designs. The maximum value of C<sub>L</sub> obtained is 0.7074 and the corresponding C<sub>D</sub> value is 0.0380 for with flaps design, while the maximum C<sub>L</sub> and C<sub>D</sub> values for without flaps design are 0.6293 and 0.0369 respectively.

**Table 7.3:- C<sub>L</sub> and C<sub>D</sub> values at different angles of attack at 15m/s (without flaps)**

WITHOUT FLAPS (v = 15 m/s)					
AOA	Lift	C <sub>L</sub>	Drag	C <sub>D</sub>	C <sub>L</sub> /C <sub>D</sub>
-5°	-0.7891	-0.2308	0.0816	0.0238	-9.6703
0°	0.9833	0.2877	0.0676	0.0197	14.5459
5°	1.2771	0.3736	0.0869	0.0254	14.6962
10°	1.8588	0.5438	0.1135	0.0332	16.3771
15°	2.1508	0.6293	0.1264	0.0369	17.0158

**Table 7.4:- C<sub>L</sub> and C<sub>D</sub> values at different angles of attack at 15m/s (with flaps)**

WITH FLAPS (v = 15 m/s)					
AOA	Lift	C <sub>L</sub>	Drag	C <sub>D</sub>	C <sub>L</sub> /C <sub>D</sub>
-5°	-	-	0.0867	0.0253	-8.7151
0°	1.2027	0.3518	0.0786	0.0229	15.3015
5°	1.7979	0.5260	0.1056	0.0308	17.0256
10°	2.1237	0.6213	0.1228	0.0359	17.294
15°	2.418	0.7074	0.1299	0.0380	18.6143



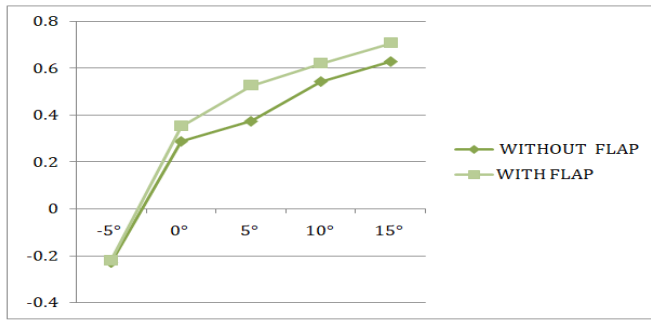


Figure 7.12:  $C_L$  vs.  $\alpha$  at 15 m/s velocity

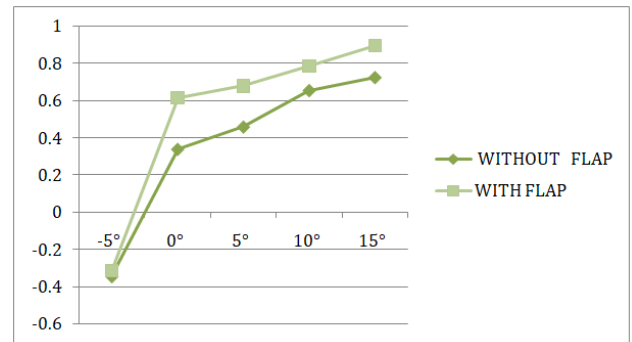


Figure 7.14:  $C_L$  vs.  $\alpha$  at 20 m/s velocity

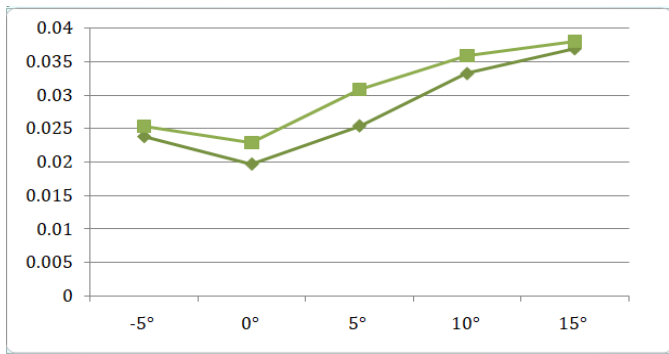


Figure 7.13:  $C_D$  vs.  $\alpha$  at 15 m/s velocity

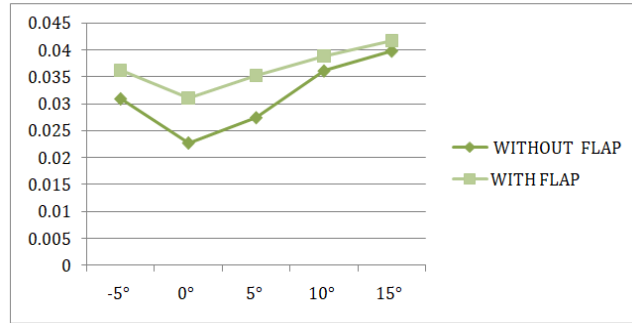


Figure 7.15:  $C_D$  vs.  $\alpha$  at 20 m/s velocity

**At 20m/s velocity**

The calculated coefficients of lift and drag values at 20 m/s velocity for without flaps and with flaps are as shown in the Table 7.15 and Table 7.16 respectively. The Figures 7.55 and 7.56 shows the comparison of both the designs. The maximum value of  $C_L$  obtained is 0.8928 and the corresponding  $C_D$  value is 0.0417 for with flaps design, while the maximum  $C_L$  and  $C_D$  values for without flaps design are 0.7228 and 0.03989 respectively.

Table 7.5:-  $C_L$  and  $C_D$  values at different angle of attack at 20m/s (without flaps)

WITHOUT FLAPS (v = 20 m/s)					
AOA	Lift	$C_L$	Drag	$C_D$	$C_L/C_D$
-5°	-2.089	-0.3438	0.1885	0.0310	-11.082
0°	2.054	0.3380	0.1389	0.0228	14.7876
5°	2.782	0.4578	0.1673	0.0275	16.6288
10°	3.9686	0.6531	0.2205	0.0362	17.9982
15°	4.3922	0.7228	0.2421	0.0398	18.1421

Table 7.6:-  $C_L$  and  $C_D$  values at different angle of attack at 20m/s (with flaps)

WITH FLAPS (v = 20 m/s)					
AOA	Lift	$C_L$	Drag	$C_D$	$C_L/C_D$
-5°	-1.8964	-0.3121	0.2204	0.0362	-8.6044
0°	3.7306	0.6139	0.1893	0.0311	19.7073
5°	4.111	0.6765	0.2143	0.0352	19.1834
10°	4.7632	0.7839	0.2364	0.0389	20.1489
15°	5.4252	0.8928	0.2534	0.0417	21.4096

Further drag polar was drawn at 20 m/s velocity. Figure 7.55 will interpret the drag polar at 20 m/s velocity. Also, the Figure 7.56 shows the plot of  $C_L/C_D$  and angle of attack ( $\alpha$ ). The maximum  $C_L/C_D$  ratio obtained is 18.1421 for without flaps BWB UAV and 21.4096 for with flaps BWB UAV, both at 15° angle of attack.

**At 25 m/s velocity:**

The calculated coefficients of lift and drag values at 25 m/s velocity for without flaps and with flaps are as shown in the Table 7.7 and Table 7.8 respectively. The Figures 7.57 and 7.58 shows the comparison of both the designs. The maximum value of  $C_L$  obtained is 1.03197 and the corresponding  $C_D$  value is 0.0429 for with flaps design, while the maximum  $C_L$  and  $C_D$  values for without flaps design are 0.8235 and 0.04219 respectively.

Table 7.7:-  $C_L$  and  $C_D$  values at different angle of attack at 25m/s (without flaps)

WITHOUT FLAPS (v = 25 m/s)					
AOA	Lift	$C_L$	Drag	$C_D$	$C_L/C_D$
-5°	-4.5784	-0.4822	0.3034	0.0319	-15.09
0°	3.5286	0.3716	0.2404	0.0253	14.678
5°	4.943	0.5206	0.2843	0.0299	17.3866
10°	6.8189	0.7182	0.3665	0.0386	18.6055
15°	7.8187	0.8235	0.3985	0.0419	19.6203

Table 7.8:-  $C_L$  and  $C_D$  values at different angle of attack at 25m/s (with flaps)

WITH FLAPS (v = 25 m/s)					
AOA	Lift	$C_L$	Drag	$C_D$	$C_L/C_D$
-5°	-3.951	-0.4161	0.3311	0.0348	-11.933
0°	6.219	0.6550	0.3034	0.0319	20.4977
5°	7.9175	0.8339	0.3685	0.0388	21.4858
10°	9.043	0.9525	0.387	0.0407	23.3669
15°	9.7973	1.0319	0.4076	0.0429	24.0366

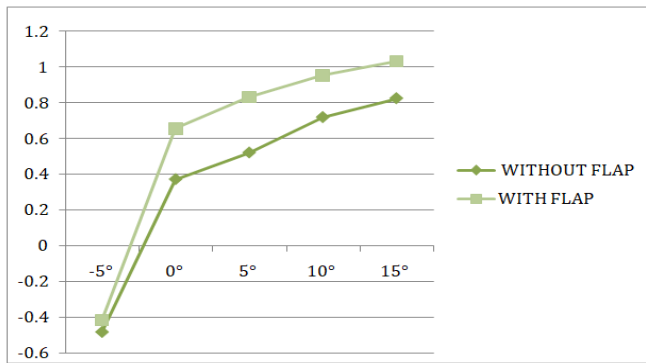


Figure 7.16:  $C_L$  vs.  $\alpha$  at 25 m/s velocity

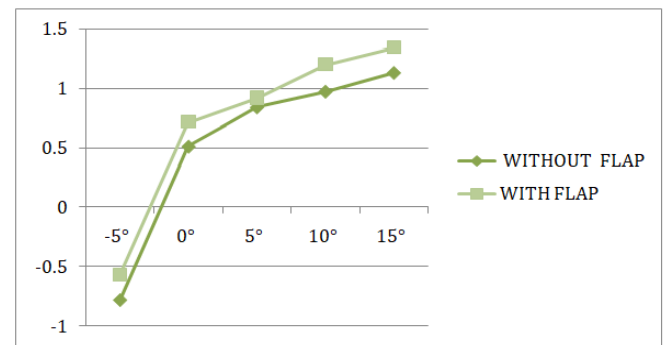


Figure 7.18:  $C_L$  vs.  $\alpha$  at 30 m/s velocity

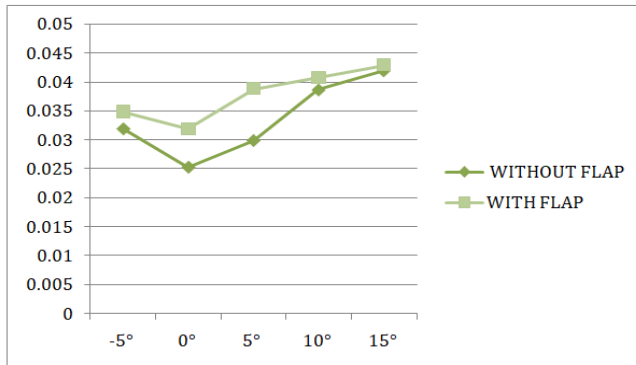


Figure 7.17:  $C_D$  vs.  $\alpha$  at 25 m/s velocity

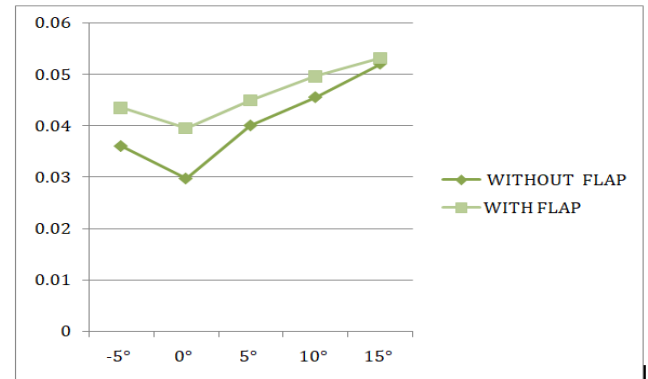


Figure 7.19:  $C_D$  vs.  $\alpha$  at 30 m/s velocity

**At 30 m/s velocity**

The calculated coefficients of lift and drag values at 25 m/s velocity for without flaps and with flaps are as shown in the Table 7.9 and Table 7.10 respectively. The Figures 7.19 and 7.20 shows the comparison of both the designs. The maximum value of  $C_L$  obtained is 1.3461 and the corresponding  $C_D$  value is 0.0531 for with flaps design, while the maximum  $C_L$  and  $C_D$  values for without flaps design are 1.1340 and 0.0520 respectively.

**Table 7.9:-  $C_L$  and  $C_D$  values at different angle of attack at 30m/s (without flaps)**

WITHOUT FLAPS ( $v = 30$ m/s)					
AOA	Lift	$C_L$	Drag	$C_D$	$C_L/C_D$
-5°	-10.751	-0.7864	0.4935	0.0360	-21.785
0°	6.9901	0.5113	0.4069	0.0297	17.1789
5°	11.5267	0.8431	0.5471	0.0400	21.0687
10°	13.3371	0.9755	0.6227	0.0455	21.4182
15°	15.504	1.1340	0.7117	0.0520	21.7845

**Table 7.10:-  $C_L$  and  $C_D$  values at different angle of attack at 30m/s (with flaps)**

WITH FLAPS ( $v = 30$ m/s)					
AOA	Lift	$C_L$	Drag	$C_D$	$C_L/C_D$
-5°	-7.7405	0.5661	0.5954	0.0435	-13.001
0°	9.8658	0.7216	0.5419	0.0396	18.2059
5°	12.6339	0.9241	0.6153	0.0450	20.5329
10°	16.449	1.2032	0.679	0.0496	24.2253
15°	18.4027	1.3461	0.7262	0.0531	25.3411

**7.4. COMPARISON OF THE RESULTS**

The lift to drag ratio (L/D) is the amount of lift generated by the wing compared to its drag. It is always best to have a greater L/D ratio. The lift producing devices such as flaps affect the production of lift which will vary with changes in angle of attack. Based on the analysis, it is seen that there is an increase in L/D ratio when flaps are added to the design, at all velocities. The Table 7.11 shows the percentage increase in L/D ratio at 15° angle of attack of the BWB UAV with flaps compared to the BWB UAV without flaps design at different velocities. The Figure 7.61 interprets the plot of L/D vs. Velocity for both the designs at 15° angle of attack.

**Table 7.11:- Comparison of L/D ratios of the two designs at 15° AOA**

Velocity (m/s)	(L/D) without flaps	(L/D) with flap	Increase in ration (%)
10	15.49	17.73	14.4609
15	17.01	18.55	9.0535
20	18.14	21.4	17.9713
25	19.62	24.03	22.4771
30	21.78	25.34	16.3453

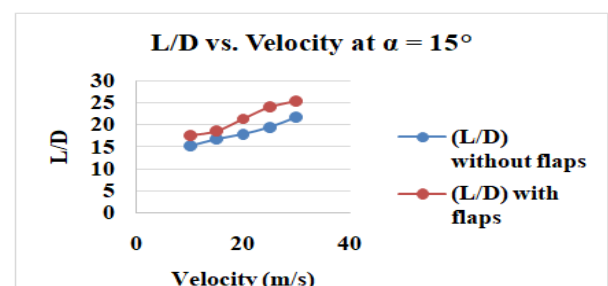


Figure 7.20: L/D vs. Velocity at 15° Angle of attack

### 8. DIFFERENT PARAMETRIC ANALYSIS

#### 8.1. PARAMETRIC ANALYSIS

Different parametric analysis is been carried out for with flap arrangement at various AOA (0°, 5°, 10°, 15°, 20°) which is by deflecting the whole BWB and by deflecting the flap at different AOA ( 5°, 10°, 15°) and then by maintaining a constant velocity of 30 m/s.

Different parametric analysis is been carried out for 0° deflection of BWB and 5°, 10°, 15° deflection of the flap.

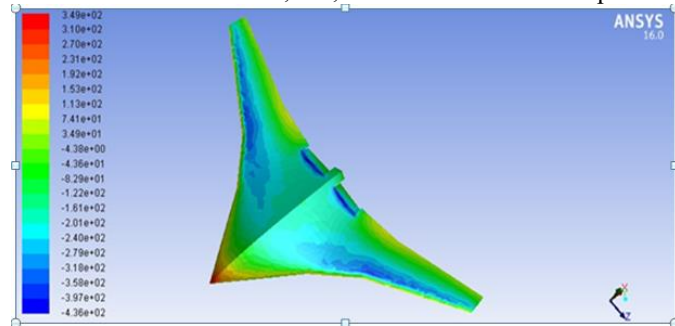


Figure 8 1: Pressure contour at 0° deflection of BWB at 5° of Flap deflection

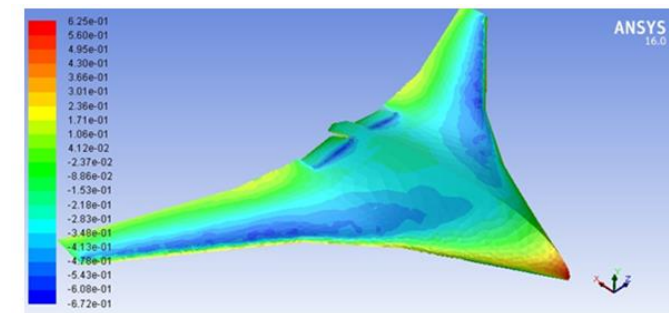


Figure8.2: Pressure contour at 0° deflection of BWB at 10° of Flap deflection

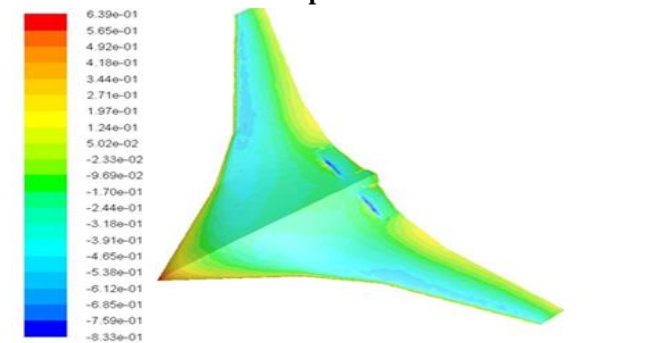


Figure8.3: Pressure contour at 0° deflection of BWB at 15° of Flap deflection

Table 8.1:- CL, CD values for 0° AOA BWB at various flap deflection

AOA	CL	CD	CL/CD
5	0.2132	0.0227	9.3537
10	0.277	0.0259	10.6826
15	0.2216	0.0199	11.1214

Different parametric analysis is been carried out for 5° deflection of BWB and 5°, 10°, 15° deflection of the flap.

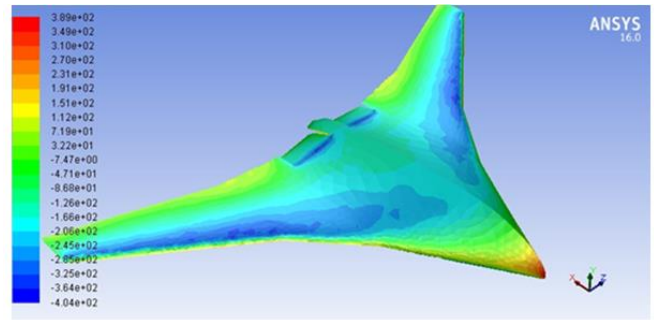


Figure8.4: Pressure contour at 5° deflection of BWB at 5° of Flap deflection

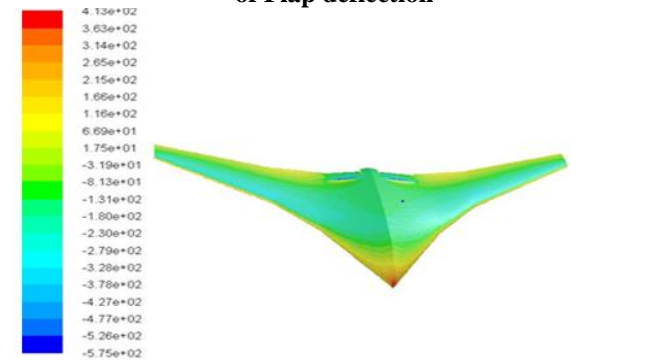


Figure8.5: Pressure contour at 5° deflection of BWB at 10° of Flap deflection

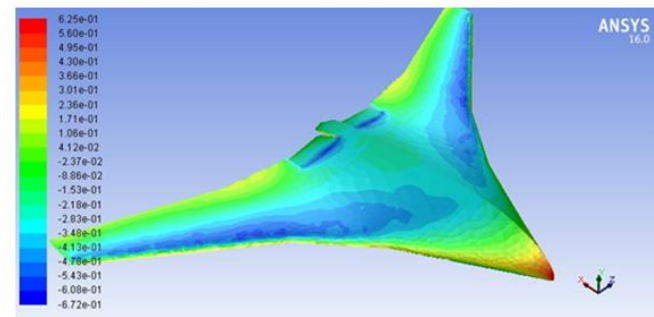


Figure8.6: Pressure contour at 5° deflection of BWB at 15° of Flap deflection

Table 8.2:- CL, CD values for 5° AOA BWB at various flap deflection

AOA	CL	CD	CL/CD
5	0.3765	0.03103	12.1334
10	0.3956	0.0323	12.2325
15	0.445	0.0341	13.0155

Different parametric analysis is been carried out for 10° deflection of BWB and 5°, 10°, 15° deflection of the flap.

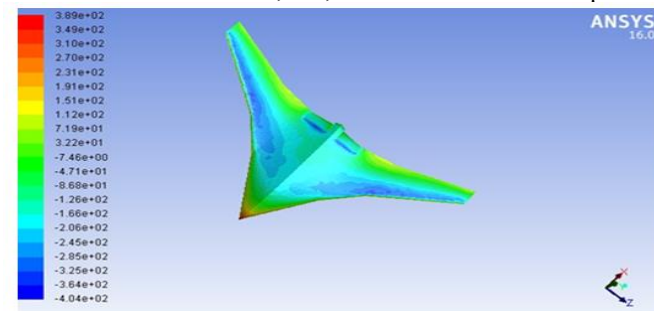


Figure8.7: Pressure contour at 10° deflection of BWB at 5° of Flap deflection



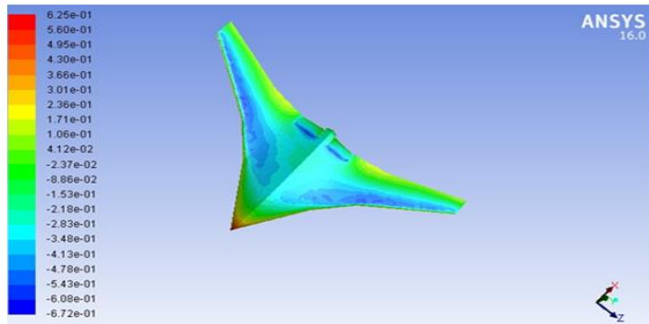


Figure 8.8: Pressure contour at 10° deflection of BWB at 10° of Flap deflection

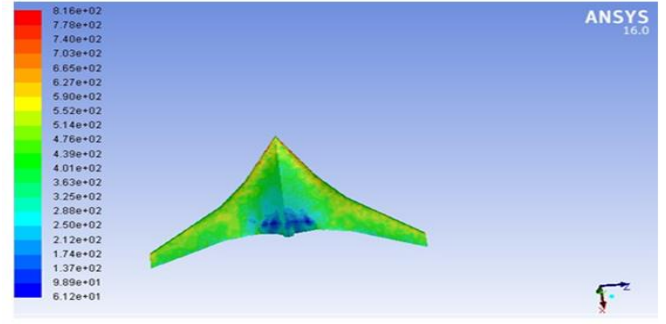


Figure 8.12: Pressure contour at 15° deflection of BWB at 15° of Flap deflection

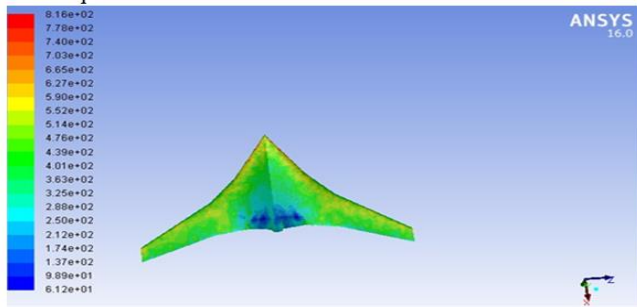


Figure 8.9: Pressure contour at 5° deflection of BWB at 15° of Flap deflection

Table 8.3:- CL, CD values for 10° AOA BWB at various flap deflection

AOA	CL	CD	CL/CD
5	0.4787	0.037	12.9378
10	0.519	0.0386	13.44
15	0.5387	0.0391	13.7669

Different parametric analysis is been carried out for 15° deflection of BWB and 5°, 10°, 15°, 20° deflection of the flap.

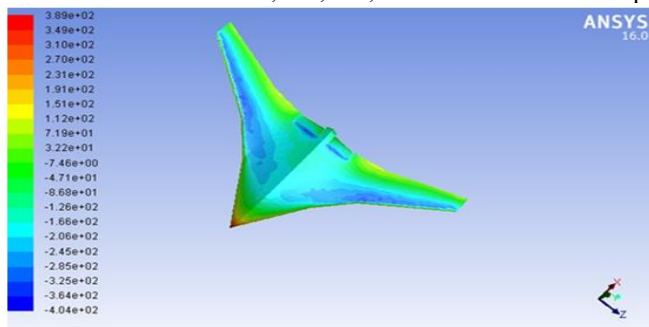


Figure 8.10: Pressure contour at 15° deflection of BWB at 5° of Flap deflection

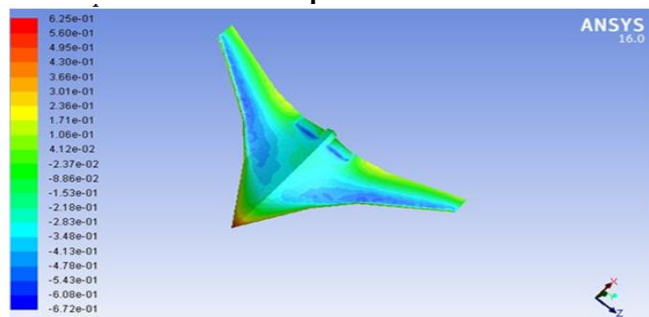


Figure 8.11: Pressure contour at 15° deflection of BWB at 10° of Flap deflection

Table 8.4:- CL, CD values for 15° AOA BWB at various flap deflection

AOA	CL	CD	CL/CD
5	0.5872	0.0398	14.7523
10	0.5998	0.0403	14.8851
15	0.6553	0.0431	15.2411

Different parametric analysis is been carried out for 20° deflection of BWB and 5°, 10°, 15° deflection of the flap.

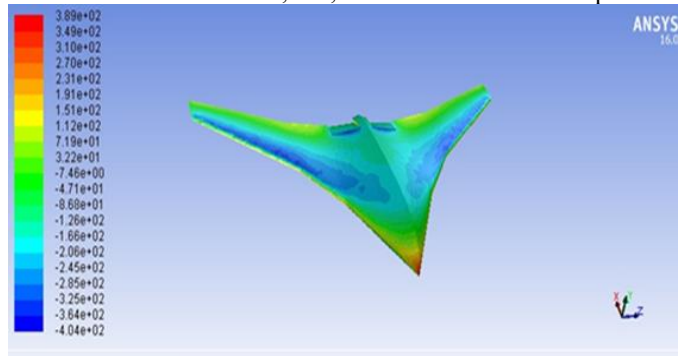


Figure 8.13: Pressure contour at 20° deflection of BWB at 5° of Flap deflection

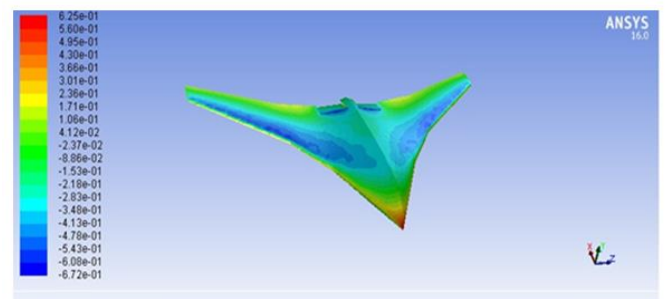


Figure 8.14: Pressure contour at 20° deflection of BWB at 10° of Flap deflection

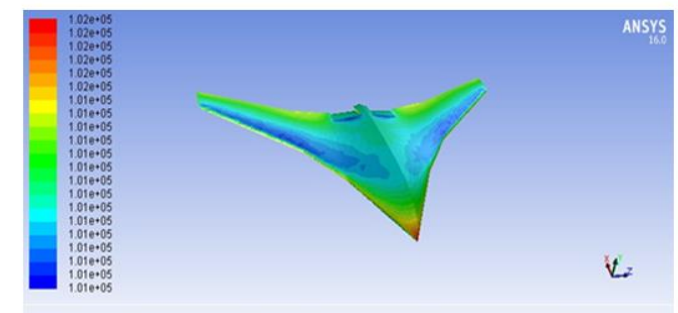


Figure 8.15: Pressure contour at 20° deflection of BWB at 15° of Flap deflection

**Table 8.5:- CL, CD values for 20° AOA BWB at various flap deflection**

AOA	CL	CD	CL/CD
5	0.9241	0.0458	20.5355
10	1.2032	0.0496	24.2580
15	1.3461	0.0531	25.3502

By working out the different parametric analysis conducted for different AOA we observed that at 20° AOA of BWB UAV at 15° deflection of flap gives the best CL/CD value of 25.35. There by we can understand that as we increase the AOA there will be increase in the generation of lift.

## 9. CONCLUSION AND FUTURE SCOPE

### 9.1. CONCLUSION

From the results, L/D ratio obtained for the BWB UAV with flaps offers a maximum value of 25, which is far greater than that of conventional aircraft that have a maximum of around 16. Flaps indeed increase the lift produced in comparison to the without flaps design. This increase in lift is due to the rise within the difference within the pressure values on the lower and upper surfaces of the BWB. By understanding the various parametric analysis conducted for various AOA we observed that at 20° AOA of BWB UAV at 15° deflection of flap gives the greater CL/CD value of 25.35. There by we will understand that as we increase the AOA there'll be increase within the generation of lift. Also, the planning with flaps features a greater L/D ratio in comparison to without flaps design. A greater or more favorable L/D ratio is usually one among the main goals of aircraft design; since a specific aircraft's required lift is about by its weight, delivering that lift with lower drag is extremely desirable.

### 9.2. FUTURE SCOPE

- The model can be tested experimentally in the wind tunnel to validate the analytical results.
- Flaps can be analyzed and tested at different deflection angles. But using the combination of leading and trailing edge high lift devices, it is possible to reduce the drag.
- Future work might include developing a supersonic BWB UAV with the combination of leading and trailing edge high lift devices.
- Performance parameters like stall speed can be calculated for the BWB UAV.

## REFERENCES

[1] Baig AZ, Cheema TA, Aslam Z, Khan YM, Sajid Dar H and Khaliq SB, "A New Methodology for Aerodynamic Design and Analysis of a Small Scale Blended Wing Body", January 2018, Journal of Aeronautical and Aerospace Engineering .

[2] Sanjiv Paudel, Shailendra Rana, Saugat Ghimire, Kshitiz Kumar Subedi, Sudip Bhattarai, "Aerodynamic and Stability Analysis of Blended Wing Body Aircraft", 2016.

[3] Martin Masereel, "Improvement of the aerodynamic behavior of a blended wing body unmanned aerial vehicle", 2016, University of Liege.

[4] Paulinus Peter Chukwuemeka Okonkwo "Conceptual Design Methodology for Blended Wing Body Aircraft", May 19, 2016, school of Aerospace Transport and Manufacturing.

[5] Melvin Philip, Venkatesh Kusnur, Prashant Manvi, "Design Optimization Of A Ducted Fan Blended Wing Body UAV Using CFD Analysis", September 2015, International Journal of Engineering and Technical Research.

[6] Pranav Mahamuni, A. Kulkarni, Yash Parikh, Aerodynamic Study of Blended Wing Body", January 2014, International Journal of Applied Engineering Research.

[7] Olverio Esteban velazquez Salazar, Julien Weiss, Francois Morency, "Development of blended wing body aircraft design", January 2015, on conference:- CASI 62<sup>nd</sup> Aeronautical conference and AGM.

[8] Midhun Mv, Partha Modal, Pwan Kumar Karn, Priyank Kumar, "Numerical and Experimental Investigation of Blended Wing Body Configuration", on August 2019.

[9] Matthew Marino, Obaid Siddique, Roberto Sabatini, "Benefits of blended wing body aircraft compared to current airliner", June 2015, on Conference: First International Symposium on sustainable Aviation.

[10] Praveen Ekka, "A Review Paper on Unmanned Aerial Vehicle (U.A.V.)" by Department of Electronics & Communication Vivekananda Institute of Technology, Jaipur, India, on April 2017, on International Journal of Research in Engineering and Technology.

[11] Shreya G, Vinitha G, Isha G, Shreya M, "Computational Analysis Blended wing Body With And Without Flaps", on 2020, in International Journal of Research in Engineering and Technology.

## LIST OF ABBRIVATIONS

- BWB - Blended Wing Body
- UAV - Unmanned Aerial Vehicle
- AOA - Angle of Attack
- CFD - Computational Fluid Dynamics
- $\alpha$  - Angle of attack
- Cl - Coefficient of lift for an airfoil
- Cd - Coefficient of drag for an airfoil
- CL - Coefficient of Lift for BWB UAV
- CD - Coefficient of Drag for BWB UAV
- L - Lift force
- D - Drag force
- S - Surface Area
- $\rho$  - Density of Air
- v - Velocity